Laser cooling of ^{173}Yb for isotope separation and precision hyperfine spectroscopy

Dipankar Das and Vasant Natarajan[*]

Department of Physics, Indian Institute of Science, Bangalore 560 012, India
(Received 7 August 2007; published 13 December 2007)

The hyperfine transitions in the 399 nm $^1S_0 \leftrightarrow {}^1P_1$ line in ^{173}Yb overlap with the transition in ^{172}Yb. We use transverse laser cooling on this line to selectively deflect ^{173}Yb atoms from a thermal beam containing both isotopes. We then use an acousto-optic modulator to span the frequency difference between the hyperfine transitions, and hence measure hyperfine structure in the $^1P_1$ state. Our precise values for the hyperfine constants, $A_{173} = 57.693 \pm 0.006$ MHz and $B_{173} = 609.028 \pm 0.056$ MHz, improve previous values significantly.

PACS number(s): 32.10.Fn, 32.80.Lg, 28.60.+s, 32.30.Jc

I. INTRODUCTION

Laser cooling is now a standard tool for creating an ultra-cold cloud of atoms [1]. Laser-cooled atoms form the starting point for a wide variety of experiments such as precision spectroscopy, atom interferometry, atomic clocks, study of ultracold collisions, and Bose-Einstein condensation. In our laboratory, we have been interested in using the advantages of cold atoms for high-resolution spectroscopy [2]. For example, Natarajan has recently proposed [3] that cold ^{171}Yb atoms launched in an atomic fountain could be used for a sensitive search of a permanent electric dipole moment (EDM) in an atom. In addition, laser-cooled Yb is an attractive species for experiments in Bose-Einstein condensation [4], photoassociation spectroscopy [5], and future all-optical clocks [6]. Many of these experiments require advanced theoretical calculations for proper interpretation of the experiments. Hyperfine spectroscopy forms an important link in such calculations since it helps in fine-tuning the atomic wave function, particularly due to contributions from nuclear interactions. Thus, precision hyperfine spectroscopy should play a direct role in understanding the implications of ongoing atomic EDM [3] and parity-violation [7] experiments.

In earlier work [8,9], we have done high-precision measurements of the frequencies of the 399 nm, $^1S_0 \leftrightarrow {}^1P_1$ line in all the stable isotopes of Yb, and measured hyperfine structure in the $^1P_1$ state of the odd isotopes, ^{171}Yb and ^{173}Yb. In ^{173}Yb, measurement of hyperfine structure poses a problem because two of the hyperfine transitions overlap with the transition in ^{172}Yb. We have solved this problem earlier by using multipeak fitting of the spectrum to extract the location of the individual transitions.

In this work, we use transverse laser cooling on the 399 nm line to selectively deflect ^{173}Yb atoms from a thermal beam containing both isotopes, and then use the deflected beam for hyperfine spectroscopy without the overlapping ^{172}Yb transition. The transverse cooling scheme is advantageous for spectroscopy because it provides a *continuous* beam of isotopically pure atoms in a field-free region. This is in contrast to the use of a Yb magneto-optic trap [10] where single isotopes can indeed be trapped and cooled, but the

perturbation produced by the trapping fields [2] requires that they be turned off during the measurement. In addition, the atomic beam provides a longer observation time and a better stability of the atom number. The 399 nm line has a high photon-scattering rate, hence the atoms can be cooled and deflected over a short distance. By choosing the correct detuning for the cooling laser, we ensure that ^{173}Yb atoms get cooled while ^{172}Yb atoms get heated, so that the deflected beam is isotopically pure. We measure the hyperfine interval using our standard technique where an acousto-optic modulator (AOM) spans the frequency difference between the two transitions [11,12]. The accuracy of 36 kHz in the measurement of the interval is a factor of 5 improvement over the previous best value. We also obtain improved values for the hyperfine constants in the $^1P_1$ state of ^{173}Yb.

II. EXPERIMENTAL DETAILS

Yb has seven stable isotopes ranging from ^{168}Yb to ^{176}Yb. It has two primary transitions from the ground state: a strong line at 399 nm corresponding to the $^1S_0 \leftrightarrow {}^1P_1$ transition, and a weak intercombination line at 556 nm corresponding to the $^1S_0 \leftrightarrow {}^3P_1$ transition. In this work, we use the strong line at 399 nm, which has a natural linewidth of $\Gamma = 2\pi \times 28$ MHz. Hence, the photon scattering rate is very high, but the saturation intensity is also correspondingly high at 58 mW/cm^2.

Yb spectroscopy is done on a collimated atomic beam generated by heating a quartz oven containing natural Yb to 300 °C. The oven is placed inside a vacuum chamber maintained at a pressure below 1×10^{-8} torr with a 20 l/s ion pump. The 399 nm laser beam is generated by doubling the frequency of a ring-cavity Ti:sapphire laser (Coherent 899-21) operating near 798 nm. The frequency of the Ti:sapphire laser is stabilized to a rms linewidth of <1 MHz using a temperature-controlled reference cavity. To minimize Doppler effects, the laser beam intersects the atomic beam at right angles. In addition, optical-pumping effects are minimized by using linearly polarized light. Its intensity is chosen to be well below the saturation intensity.

As mentioned earlier, the 399 nm transition in ^{172}Yb overlaps with the $F=3/2$ and $F=7/2$ hyperfine transitions in ^{173}Yb. To separate these isotopes, we have used transverse laser cooling of the atomic beam. We then do hyperfine spectroscopy on the isotopically pure beam, and use our standard technique of locking an AOM to the frequency difference

―――――
*URL: http://www.physics.iisc.ernet.in/~vasant.   E-mail: vasant@physics.iisc.ernet.in
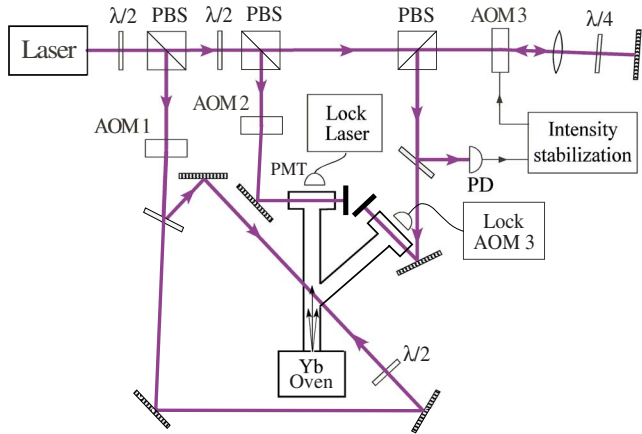
FIG. 1. (Color online) Schematic of the experiment. Figure key: AOM, acousto-optic modulator; PBS, polarizing beam splitter; $\lambda/2$, half-wave retardation plate; $\lambda/4$, quarter-wave retardation plate; PD, photodiode; PMT, photomultiplier tube.

between the two transitions to measure the hyperfine interval [11,12], where we showed that the interval can be measured with an accuracy of better than one part in 1000 of the linewidth. Such transverse laser cooling has been used earlier for deflection of an atomic beam of Ca atoms, and the cold deflected atoms were used for high-resolution spectroscopy experiments [13]. However, in contrast to the present work, only one isotope was involved and the longitudinal velocity of the atoms had to be first slowed using a Zeeman slower.

To perform spectroscopy on the deflected atoms, we have designed a glass chamber with two arms in a Y-shaped configuration. The undeflected atoms go into a region for fluorescence spectroscopy, which we call the main arm. The cooling beams intersect the atomic beam at a suitable angle so that the cooled atoms travel at an angle with respect to their original direction. The deflected atoms go into a side arm where we can independently address them. The cooling beams are linearly polarized and counter-propagate with respect to each other to form a one-dimensional molasses configuration. The angle and size of the cooling beams is an important consideration. First, the angle must be small enough so that the velocity component along the cooling direction is within the capture range of the molasses. Assuming a detuning of 1.1Γ, the capture velocity is about 25 m/s. The angle was chosen to be 40° so that, for an oven at 300 °C, a good fraction of atoms have velocity below 25 m/s. The size of the beams was chosen to be 8 mm with a power of 25 mW. We have shown earlier that a magneto-optic trap for Yb atoms can be loaded from thermal vapor [10] with beams of this size and power, therefore the choice is reasonable.

The experimental schematic is shown in Fig. 1. The experiment requires three distinct laser frequencies, one for the cooling and two for the hyperfine transitions. The three frequencies are generated using AOMs labeled 1, 2, and 3, respectively. The required frequencies become clear by looking at the relevant part of the spectrum, as shown in Fig. 2(a). The cooling laser frequency is chosen so that it is red detuned by 32 MHz (1.1Γ) from the ^{173}Yb $(F=7/2)$ transition, and blue detuned by 23 MHz from the ^{172}Yb transition.
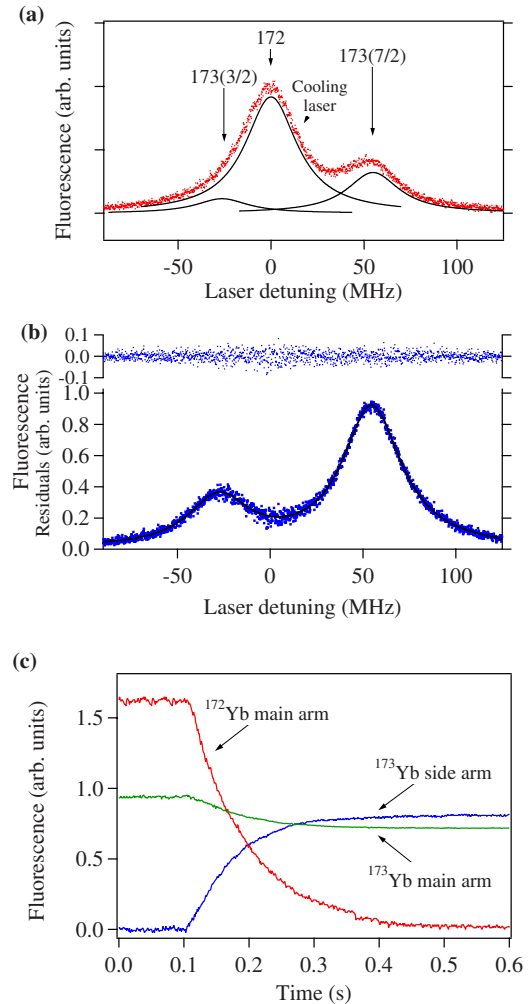

FIG. 2. (Color online) (a) The (red) dots represent the fluorescence signal in the main arm, showing the overlapping ^{172}Yb and ^{173}Yb $(F=3/2$ and $F=7/2)$ peaks. The three solid curves show the peaks as extracted from a multipeak fit to the spectrum. Also shown is the location of the cooling laser, which is red detuned for ^{173}Yb and blue detuned for ^{172}Yb. (b) The (blue) spectrum is from the side arm after isotope separation, showing the resolved ^{173}Yb peaks and the complete absence of the ^{172}Yb peak. The solid curve is a Lorentzian fit with the residuals shown on top. (c) Fluorescence levels in the two arms. The ^{172}Yb signal in the main arm goes to zero due to heating, while the ^{173}Yb signal in the side arm increases from zero due to cooling. The ^{173}Yb signal in the main arm decreases slightly as atoms get deflected.

Hence the ^{173}Yb atoms get cooled and deflected, while the ^{172}Yb atoms get heated toward the walls.

The effect of the cooling is seen clearly from the fluorescence levels shown in Fig. 2(c). As can be seen, the fluorescence from the ^{172}Yb atoms goes to zero in the main arm as the atoms get heated toward the walls. On the other hand, the fluorescence from the ^{173}Yb atoms in the side arm (on the $F=3/2$ transition) increases from zero as the atoms get cooled and deflected. At the same time, the fluorescence level from the ^{173}Yb atoms in the main arm (on the $F=7/2$ transition) goes down only slightly as some fraction of atoms get deflected. It is important that this level does not go to

zero because the error signal from this arm is used to lock the laser to the ^{173}Yb ($F=7/2$) transition. Furthermore, the complete absence of ^{172}Yb atoms in the main arm is important in ensuring that the ^{173}Yb ($F=7/2$) peak does not get pulled by the ^{172}Yb peak.

The dramatic improvement in the spectrum due to the cooling is seen in Fig. 2. The partially resolved spectrum in the main arm without the cooling beam is shown in Fig. 2(a). The spectrum is obtained by scanning the frequency-doubled Ti:sapphire laser over the three transitions. The strong ^{172}Yb transition completely swamps the ^{173}Yb ($F=3/2$) transition. This is the kind of spectrum from which, in earlier work [8,9], we had extracted the locations of the individual transitions using a multipeak fitting algorithm. Typical fits to the three peaks are shown as solid curves in the figure. The spectrum in the side arm after transverse cooling is shown in Fig. 2(b). The ^{172}Yb peak is completely absent, allowing us to observe a clearly-resolved spectrum for the two hyperfine transitions in ^{173}Yb. The spectrum is obtained by using the primary laser to produce the cooling beam, and by scanning a frequency-stabilized blue diode laser (Nichia Corporation 399 nm, 30 mW diode) in the side arm, since the limited bandwidth of the AOM does not allow such a large frequency scan. The solid curve is a two-peak Lorentzian fit and the featureless residuals show that the line shape is highly symmetric.

The experiment now proceeds as follows. The laser is first downshifted through AOM2 (by 102 MHz) and the resulting beam is used for spectroscopy on the undeflected atomic beam in the main arm of the chamber. The frequency shift of the AOM is dithered at 20 kHz (with 10 MHz depth of modulation) to generate an error signal, which is used to lock the laser on the ^{173}Yb ($F=7/2$) transition. Note that the laser frequency is 102 MHz above this transition because of the downshift through AOM2. The cooling beam is generated by downshifting the laser frequency through AOM1 (by exactly 134 MHz), so that it is 32 MHz below the ^{173}Yb ($F=7/2$) transition and 23 MHz above the ^{172}Yb transition. Finally, a third beam is generated by double passing through AOM3, set for a total downshift of about 174 MHz. This beam is thus resonant with the ^{173}Yb ($F=3/2$) transition and is used for spectroscopy on the side arm of the chamber. The shift of AOM3 is again dithered (at a slightly different frequency of 21 kHz), and the resulting error signal is used to lock the frequency of AOM3 to this transition. Thus the frequency difference of AOM2 and AOM3 directly gives the hyperfine interval between the $F=7/2$ and $F=3/2$ transitions. The double passing through AOM3 is important to maintain directional stability as the AOM frequency changes. Furthermore, the intensity of the shifted beam is stabilized by feedback control of the rf power exciting the AOM. Finally, the error signals are generated by phase-sensitive detection at the third harmonic of the modulation frequency [14]. This is known to produce narrow error signals that are free from effects due to intensity fluctuations [11], which is important since the frequency modulation of AOM2 can produce residual amplitude modulation. Note that the modulation of AOM3 will not produce amplitude modulation because the output intensity is stabilized in a servo loop.
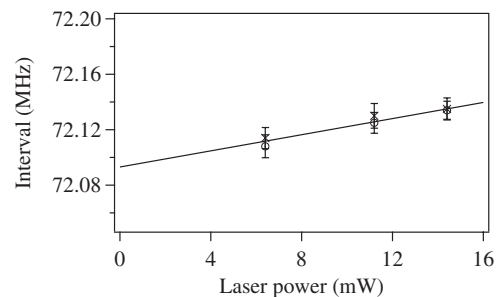

FIG. 3. The measured $F=7/2-F=3/2$ hyperfine interval in the $^1P_1$ state of ^{173}Yb is plotted against laser power to check for intensity-dependent errors. Circles and crosses are measurements on different days, and the error bars are the statistical error in each value. The solid line is a linear fit used to extrapolate to zero power.

III. RESULTS AND DISCUSSION

We now present the results of measurements of the ^{173}Yb, $F=7/2-F=3/2$ hyperfine interval. To check for intensity-dependent errors, the measurements were done at three powers of the excitation laser beams (in both arms). The $1/e^2$ size of the beam was 8 mm, so that the intensity at beam center for the highest power of 14 mW was only 31 mW/cm^2, which is still smaller than the saturation intensity of 58 mW/cm^2. At each power, we took an average of about 300–400 independent measurements. This procedure was repeated after a few days. In Fig. 3, we show the average values measured on 2 days plotted against laser power. The error bars are the statistical error in each value. There is a slight increasing trend in the data though it is smaller than the error bars. The linear fit extrapolated to zero power yields a value of 72.093 MHz for the hyperfine interval with a statistical error of 11 kHz.

The total error in the interval is obtained by adding in quadrature the different sources of error listed in Table I. The largest error is due to the Doppler shift arising from misalignment of the laser beams from perpendicularity. The error is estimated using a typical misalignment angle of 0.1 mrad. Since the measurement on the second day was done with complete realignment of the laser beams, the consistency of the two data sets gives an upper bound on this error. The other important source of error is optical pumping into Zeeman sublevels. In the presence of stray magnetic fields, there will be a shift of the sublevels, and hence a shift of the line center. With linearly polarized light, this error should be

TABLE I. Error budget.

Source of error	Size (kHz)
(1) Statistical	11
(2) Doppler shift due to misalignment from perpendicularity	30
(3) Optical pumping into Zeeman sublevels	15
(4) Laser lock to peak center (feedback loop errors)	7
(5) Collisional shifts	<5

TABLE II. Comparison of the ^{173}Yb ($F=7/2-F=3/2$) hyperfine interval in the $^1P_1$ state measured in this work to previous measurements from our laboratory.

Interval (MHz)	Reference
72.093 ± 0.036	This work
72.011 ± 0.207	[8]
72.740 ± 1.006	[9]

negligible. However, there could be residual ellipticity of the beams, due to birefringence at the windows, for example. The error is estimated by assuming an ellipticity of 5% and a stray magnetic field of 100 mG.

We have considered other sources of error such as radiation-pressure shifts, the ac Stark shift, and peak pulling due to the neighboring hyperfine transition. The common feature of all these errors is that they increase with laser power. (i) Radiation pressure causes velocity redistribution of the atomic beam which could lead to asymmetry of the line shape. However, to the extent that the scattering rate is the same in both arms (since the same laser power is used), the distortion should be similar and should cancel in the difference measurement. More importantly, the scattering rate should increase when the laser power is increased. (ii) The ac Stark shift averages to zero for a one-photon transition on resonance, but there could be some residual effect due to the nearby hyperfine level from which the laser is detuned. Again, the Stark shift should increase with the laser power. (iii) Finally, errors due to peak pulling from the neighboring transition should be minimized by the use of third-harmonic locking. However, the size of the error can be significant at the kHz level. For the spectrum shown in Fig. 2(b), the separation of the third-derivative zeroes of the Lorentzian fit is 39 kHz more than the separation of the peaks. Again, the amount of peak pushing will increase with the spectral linewidth, and the linewidth in turn will increase with laser power due to power broadening of the transition.

Thus all of the above sources of error should increase with laser power. This is why we have done the measurement at three powers. The maximum shift of the interval in Fig. 3 is of order 40 kHz, which indicates that the peak-pulling effect probably makes the largest contribution. In any case, the value extrapolated to zero power should be free of the above errors. The final error taking into account the other sources of error listed in Table I is 36 kHz.

As mentioned earlier, we have previously measured this interval in our laboratory using a multipeak fit to the overlapping spectrum [8,9]. We compare the result from the present work to these previous values in Table II. As can be seen, the three results overlap with each other within 1σ, but the present measurement represents more than a factor of 5 improvement in precision. We can combine this value with the value of 841.404 ± 0.070 MHz for the ^{173}Yb, $F=7/2-F=5/2$ hyperfine interval reported in our earlier work [8], to obtain the hyperfine constants in the $^1P_1$ state,
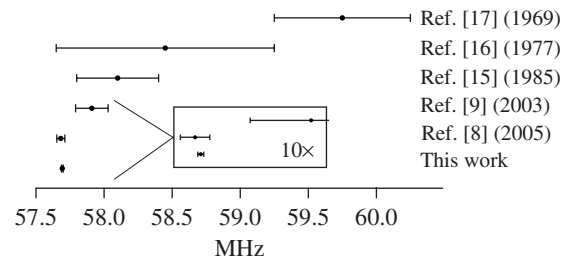
$$A_{173} = 57.693 \pm 0.006 \text{ MHz},$$

TABLE III. Comparison of measurements of hyperfine constants in the $^1P_1$ state of ^{173}Yb. The first three measurements are all from our laboratory.

Hyperfine constant (MHz)		
A_{173}	B_{173}	Reference
57.693 ± 0.006	609.028 ± 0.050	This work
57.682 ± 0.029	609.065 ± 0.098	[8]
57.910 ± 0.120	610.470 ± 0.840	[9]
58.10 ± 0.3	588.0 ± 2	[15]
58.45 ± 0.8	589.6 ± 13	[16]
59.75 ± 0.5	604.0 ± 7	[17]
	605.0 ± 20	[18]

$$B_{173} = 609.028 \pm 0.056 \text{ MHz}.$$

These values are compared to previously published values in Table III, and shown as a deviation plot in Fig. 4. Over the years, hyperfine structure in the $^1P_1$ state of ^{173}Yb has been measured using techniques such as level crossing-anticrossing spectroscopy [15–17] and use of a Fabry-Perot cavity [18]. However, all of these measurements have large error bars. The three recent high-precision measurements are all from our laboratory. The small error bars for these measurements become clear in the expanded view shown in the figure insets. Comparing to the other values, we see that the value for A is quite consistent with the previous results. The value of B is also in agreement with all the previous values

(a) Hyperfine constant A_{173}
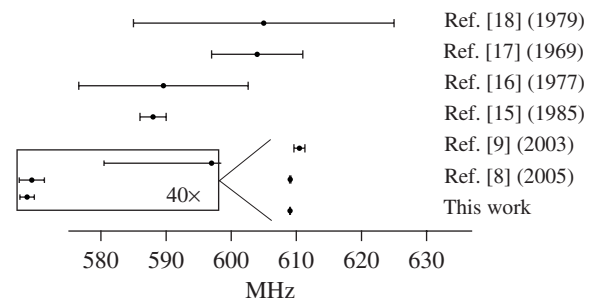

(b) Hyperfine constant B_{173}

FIG. 4. Comparison of hyperfine constants in the $^1P_1$ state of ^{173}Yb measured in this work to results from previous measurements. The bottom three measurements are all from our laboratory. The error bars for these measurements become clear in the expanded view shown in the insets.

except for the low value reported by Liening [15] from a level crossing experiment. Our present work represents a significant improvement in precision over our earlier work [8], by factors of 5 and 2, respectively.

IV. CONCLUSION

In conclusion, we have used transverse laser cooling of an atomic beam for separating two isotopes of Yb, ^{172}Yb and ^{173}Yb. By proper choice of the cooling frequency, the desired isotope ^{173}Yb gets cooled and deflected into the side arm, while the unwanted isotope ^{172}Yb is heated toward the walls. We are thus able to selectively address the hyperfine transitions in ^{173}Yb, which otherwise overlap with the transition in ^{172}Yb. We then use an AOM to measure the hyperfine interval with high precision. The hyperfine constants in the $^1P_1$ state thereby obtained have the highest accuracy to date. The transverse laser cooling method should have general applications in other atoms for isotope separation and isotope-selective spectroscopy.

[1] A good review of laser cooling experiments is contained in the Nobel Prize lectures: S. Chu, Rev. Mod. Phys. **70**, 685 (1998); C. N. Cohen-Tannoudji, *ibid.* **70**, 707 (1998); W. D. Phillips, *ibid.* **70**, 721 (1998).

[2] U. D. Rapol, A. Wasan, and V. Natarajan, Europhys. Lett. **61**, 53 (2003).

[3] V. Natarajan, Eur. Phys. J. D **32**, 33 (2005).

[4] Y. Takasu, K. Honda, K. Komori, T. Kuwamoto, M. Kumakura, Y. Takahashi, and T. Yabuzaki, Phys. Rev. Lett. **90**, 023003 (2003).

[5] S. Tojo, M. Kitagawa, K. Enomoto, Y. Kato, Y. Takasu, M. Kumakura, and Y. Takahashi, Phys. Rev. Lett. **96**, 153201 (2006).

[6] Z. W. Barber, C. W. Hoyt, C. W. Oates, L. Hollberg, A. V. Taichenachev, and V. I. Yudin, Phys. Rev. Lett. **96**, 083002 (2006).

[7] J. E. Stalnaker, D. Budker, S. J. Freedman, J. S. Guzman, S. M. Rochester, and V. V. Yashchuk, Phys. Rev. A **73**, 043416 (2006).

[8] D. Das, S. Barthwal, A. Banerjee, and V. Natarajan, Phys. Rev. A **72**, 032506 (2005).

[9] A. Banerjee *et al.*, Europhys. Lett. **63**, 340 (2003).

[10] U. D. Rapol, A. Krishna, A. Wasan, and V. Natarajan, Eur. Phys. J. D **29**, 409 (2004).

[11] U. D. Rapol, A. Krishna, and V. Natarajan, Eur. Phys. J. D **23**, 185 (2003).

[12] D. Das and V. Natarajan, Eur. Phys. J. D **37**, 313 (2006).

[13] A. Witte, T. Kisters, F. Riehle, and J. Helmcke, J. Opt. Soc. Am. B **9**, 1030 (1992).

[14] A. J. Wallard, J. Phys. E **5**, 926 (1972).

[15] H. Liening, Z. Phys. A **320**, 363 (1985).

[16] M. Baumann, H. Liening, and H. Lindel, Phys. Lett. **59A**, 433 (1977).

[17] B. Budick and J. Snir, Phys. Rev. **178**, 18 (1969).

[18] P. Grundevik, M. Gustavsson, A. Rosen, and S. Rydberg, Z. Phys. A **292**, 307 (1979).